PROCEEDINGS, 41st Workshop on Geothermal Reservoir Engineering
Stanford University, Stanford, California, February 22-24, 2016
SGP-TR-209

# Investigating the Possibility of Using Tracer Tests for Early Identification of EGS Reservoirs Prone to Flow Channeling

Bin Guo, Pengcheng Fu, Yue Hao, Charles R. Carrigan

Atmospheric, Earth, and Energy Division, Lawrence Livermore National Laboratory

P.O. Box 808, Livermore, CA 94551-0808

fu4@llnl.gov

**Keywords:** EGS, flow channeling, tracer test

## ABSTRACT

Channelized flow due to inherent heterogeneity in fracture aperture fields and further flow channeling caused by thermo-mechanical effects can substantially reduce the effective heat exchange area of fractures and thereby cause inferior performance of EGS reservoirs. Our previous studies have identified that initially channelized flow fields tend to have greater additional channeling than initially diffuse flow fields do. The current work investigates the possibility of identifying EGS reservoirs that enable highly channelized flow fields so that we can optimize production strategy. Based on a coupled Thermo-Hydro-Mechanical model that we had developed to simulate flow channeling in EGS dominated by a single fracture, we developed a conservative tracer module that can be used to quantify the tracer signature of the EGS at any given time in its heat production life cycle. We simulated tracer tests performed on the initial flow fields of hundreds of randomly generated fracture aperture fields for which the heat production performance had been quantified in a previous study. By quantifying the correlations between various tracer response metrics and EGS heat production lives, we found that the highest peak concentration and mean residence time of tracer tests can be used to identify flow systems that will lead to very short production lives. However, these tracer response metrics seem to be unable to differentiate flow systems with very good performance from those with intermediate performance if only conservative tracer is used.

## 1. INTRODUCTION

Flow channeling along flow-carrying fractures can significantly undermine heat production performance (Fu et al. 2015) of engineered (or enhanced) geothermal systems (EGS). Because of the ubiquitous heterogeneity in subsurface formations, flow along fractures, including natural fractures and man-made hydraulic fractures, is inevitably channelized, and the channelization of flow can be aggravated by thermo-hydro-mechanical processes during heat production (Tsang and Tsang 1989; Tsang and Tsang 1989; Tsang and Neretnieks 1998; Fu et al. 2015; Guo et al. 2016). Flow channeling can severely reduce the effective heat exchange area, and thereby the heat production life of an EGS. Our previous work had found that in an EGS dominated by a single fracture, the spatial variation of the aperture alone, even when the mean aperture, the standard deviation of the aperture, and the auto-correlation length of the aperture field remain the same, can cause the effective production life to vary from less than 5 years to beyond 30 years (Guo et al. 2016). It is therefore highly desirable to identify aperture fields that are prone to flow channeling at an early stage.

Tracer tests are a powerful diagnostic tool for studying reservoir properties, such as inter-well hydraulic connections, that are otherwise impossible to characterize. They have been widely used in subsurface contamination treatment, nuclear waste disposal, oil and gas extraction, etc. (Horne 1985; Gale et al. 1987; Hadermann and Heer 1996; McGuire et al. 2005). Multiple compounds can be used as tracers, and they can be divided into conservative/non-reactive tracers and reactive tracers. In EGS reservoirs, conservative tracers, matrix sorptive tracers, thermo-sensitive tracers, and partitioning tracers are commonly used for the purpose of quantifying heat exchange between the working fluid and rock matrix (Rose et al. 2001; Bloomfield and Moore 2003; Wu et al. 2008; Nottebohm et al. 2012; Maier et al. 2015). The analysis of tracer tests data in the Laugaland geothermal field in Iceland identified two tracer transport modes: transport through direct, small-volume paths and transport through dispersion and mixing in a large volume (Axelsson et al. 2001). The tracer tests conducted at Soultz-sous-Forêts geothermal site in France showed evidence of good hydraulic connection between the injection well and one production well, as well as poor communication between the injection well and the other production well (Sanjuan et al. 2006). The applications of tracer tests to various EGS sites (Hadermann and Heer 1996; Kumagai et al. 2004; Radilla et al. 2012; Ayling et al. 2015) have also proven that tracer tests are practically feasible and informative of the flow field.

In this study, we investigate the possibility of using tracer tests to identify aperture fields that encourage flow channeling and thereby are prone to poor heat production performance. As a proof-of-concept study, the current work is based on 200 virtual aperture fields randomly generated for a large fracture that serves as the sole heat exchange surface of an idealized EGS (Guo et al. 2016). The 200 aperture fields cover a variety of aperture correlation lengths and aperture standard deviations, and multiple stochastic realizations were generated for each parameter combination. In that study, the effects of flow channeling on EGS heat production were studied using a thermo-hydro-mechanical (THM) model developed on LLNL's GEOS simulation framework. Those heat production performance data are directly used in the current work. In this study, we developed a tracer transport model on the same simulation platform, GEOS, to study the tracer signatures of these 200 virtual systems. We limit the current investigation to an idealized conservative trace, namely a compound that neither reacts with nor gets absorbed by the rock formation. We also only study the system's responses to tracer pulses in an early stage of heat production when THM coupling has not significantly altered the initial flow field yet. In other words, when the tracer test is performed, the system could and is likely to have channelized flow due to the natural heterogeneity in the aperture field but the channelization has not been exacerbated by THM coupling yet. Even though tracer tests at a later production stage could correlate

with heat production performance better, such an after-the-fact diagnosis is much less useful than an early prediction before the electricity generation facilities have been constructed.

## 2. TRACER TRANSPORT MODEL

Based on the THM model we developed on GEOS, a tracer transport model was developed using a finite volume formulation. The governing equation of tracer transport in porous medium is

$$\frac{\partial C}{\partial t} = -\frac{\mathbf{u}}{\phi}\nabla C + \nabla \cdot (D \nabla C) + S \tag{1}$$

where $C$ is the volumetric concentration of the tracer; $t$ is time; $\mathbf{u}$ is the apparent fluid velocity vector; $\phi$ is porosity; $D$ is the dispersion coefficient of tracer; and $S$ is the source/sink term. Integrate Equation (1) over a representative element volume

$$\int \frac{\partial C}{\partial t} dV = -\int \frac{\mathbf{u}}{\phi}\nabla C dV + \int \nabla \cdot (D \nabla C) dV + \int S dV \tag{2}$$

By assuming tracer is well-mixed in each cell and applying Green's theorem, the above equation can be rewritten as

$$\frac{\partial C}{\partial t}\Delta V = -\int_{\Gamma} \frac{\mathbf{u} C}{\phi} \cdot \mathbf{n}\, d\Gamma + \int_{\Gamma} D \nabla C \cdot \mathbf{n}\, d\Gamma + S \Delta V \tag{3}$$

where $\mathbf{n}$ is a unit vector perpendicular to the boundary of REV. Velocity vector $\mathbf{u}$ is calculated by Darcy's law

$$\mathbf{u} = -\frac{\mathbf{k}}{\mu}(\nabla P - \rho \mathbf{g}) \tag{4}$$

where $\mathbf{k}$ is the permeability tensor; $\mu$ is the dynamic viscosity; $P$ is the pressure; $\rho$ is the fluid density; and $\mathbf{g}$ is the gravity acceleration vector. Substituting equation (4) into equation (3) yields

$$\frac{\partial C}{\partial t}\Delta V = \int_{\Gamma} \frac{\mathbf{k}}{\mu \phi}(\nabla P - \rho \mathbf{g}) C \cdot \mathbf{n}\, d\Gamma + \int_{\Gamma} D \nabla C \cdot \mathbf{n}\, d\Gamma + S \Delta V \tag{5}$$

Similar to the THM model, the simulation domain is discretized into 3D 8-node hexahedron elements, and a fracture is represented by a thin layer of porous medium with an equivalent porosity. The equivalent porosity of a fracture cell is calculated by

$$\phi = \frac{A}{T} \tag{6}$$

where $A$ is the fracture aperture; and $T$ is the thickness of the thin layer that represents fracture.

We use upwind scheme for the advection term in equation (5), because the advection term is dominant compared with the dispersion term in our system. The time-step is controlled by the cell that has the minimum time step to satisfy stability requirement.

## 3. TRACER TESTS

### 3.1 Single-fracture system

Similar to our previous study of flow channeling due to THM processes, the tracer tests are performed in an EGS reservoir with an engineered fracture as the primary connection between an injection well and a production well (Hogarth and Bour 2015; Llanos et al. 2015). The fracture is horizontal because the minimum principal stress is in vertical direction. It is assumed to be a penny-shaped fracture with a diameter of 1,000 m at a depth of 3,000 m. The distance between the injection and production wells is 500 m. The fracture is represented by the 2 mm thick layer of porous medium. Figure 1 shows the single-fracture system. Refer to Table 1 in (Guo et al. 2016) for the rock properties and fluid properties.

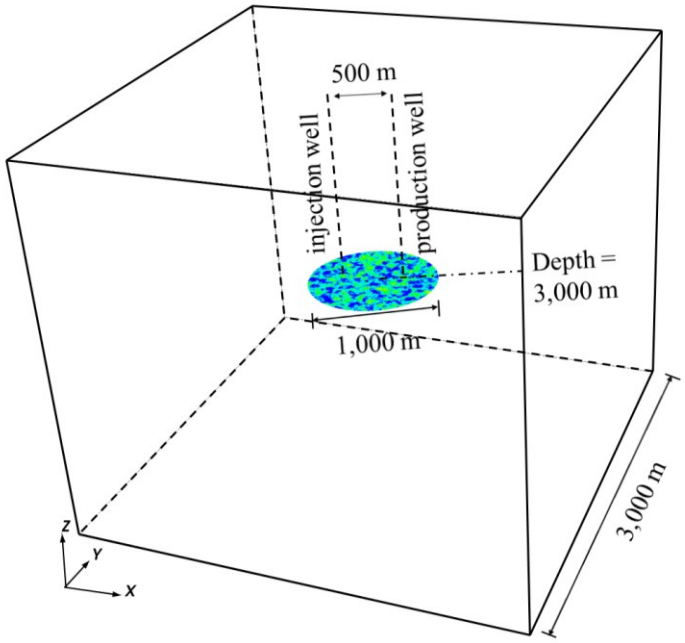


**Figure 1: Single-fracture system**

The downhole pressure in the production well at the depth of the fracture is kept as the same with initial pore pressure (34 MPa) and we fix the injection rate of 12.5 liter/s at the injection well. We apply a zero-flux boundary condition and "roller" boundary condition at the far-field boundaries.

### 3.2 Spatial heterogeneity in aperture field

We use correlation length and standard deviation to quantify spatial heterogeneity of the aperture field, as is described in (Guo et al. 2016). Table 1 shows the design of combinations of correlation length and standard deviation in this study. We first change correlation length while keeping the same standard deviation in Set 1, and then change the standard deviation using the same correlation length in Set 2. In Set 2, we use the longest correlation length because we found that standard deviation affects flow channeling only when the correlation length is long in (Guo et al. 2016). We perform 20 tracer test realizations for each combination of correlation length and standard deviation to make the results statistically representative. We also run one realization with a homogeneous aperture field as the base case.

**Table 1: Design of spatial heterogeneity of aperture field**

| | Correlation length (m) | Standard deviation (mm) | Number of realizations |
|---|---|---|---|
| Set 1: varying correlation length | 12.5 | 0.17 | 20 |
| | 25 | 0.17 | 20 |
| | 50 | 0.17 | 20 |
| | 100 | 0.17 | 20 |
| | 200 | 0.17 | 20 |
| Set 2: varying standard deviation | 200 | 0.0425 | 20 |
| | 200 | 0.085 | 20 |
| | 200 | 0.17 | 20 |
| | 200 | 0.34 | 20 |
| | 200 | 0.68 | 20 |

### 3.3 The tracer test simulation

Two time-scales associated with a tracer test play significant roles in determining the outcomes and analysis of the test. The first is the tracer injection duration and the second is the residence time of the injected tracer in the reservoir. If the former is significantly shorter than the latter, the injection can be considered a short "pulse", making the analysis of the results relatively simple. In our study, the injection duration is chosen to be 10 minutes whereas the mean residence time is typically between 1 hour and 3 hours for the simulated system, so this condition applies. Moreover, if the tracer residence time is much shorter than the time scale within which significant flow field evolution can occur, the flow system can be assumed to be in a steady state within the tracer simulation window and a snapshot of the flow velocity field can be used for the simulation. Based on our previous work (Guo et al. 2016), the evolution of the flow field caused by THM coupling only becomes significant over a time span of at least months. Therefore, we only need to run the THM model for a relatively short period of time (1 hour typically) so that the flow reaches a semi-steady state, which is defined as a state where flow transience is negligible for time scales of hours to days. We then simulate tracer injection at a concentration of 1.0 $mol/m^3$ for 10 minutes and subsequently run tracer transport model for 48 hours after which the produced tracer concentration is minimal (less than $10^{-4}$ of the injected tracer concentration).

## 4. RESULTS

### 4.1 Tracer transport results of a representative realization

Figure 2 shows a series of snapshots of the tracer concentration field at different times. We use the middle of the tracer injection as the reference time, i.e. t = 0. At t = 5 min, tracer injection ends and the injected tracer are close to the injection well. As the transport process progresses, tracer is diluted due to advection, dispersion, and mixing in each cell. The last moment that we include in the figure is t = 15 hours, beyond which tracer concentration becomes too low to visually detect.

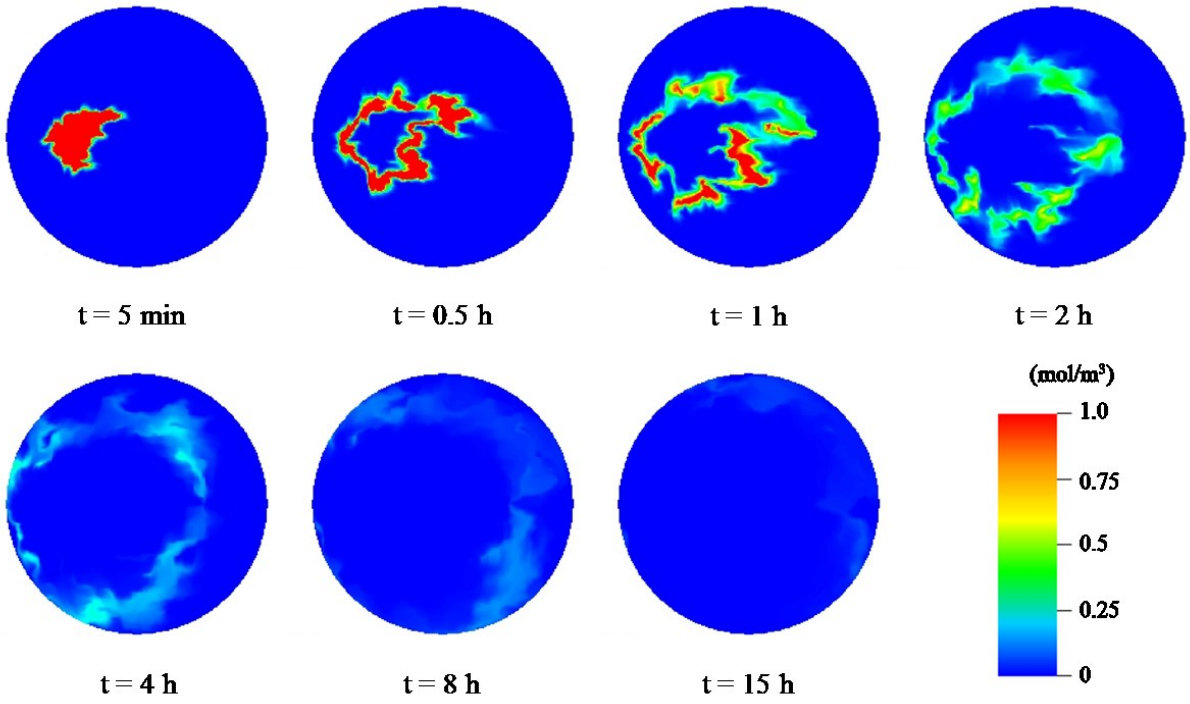


**Figure 2: Tracer field evolution for one realization with correlation length of 50 m and standard deviation of 0.17 mm.**

Figure 3 shows the tracer concentration measured at the production well, called tracer response curve, from one realization of the aperture field with a correlation length of 50 m and standard deviation of 0.17 mm. The corresponding aperture, flow rate, and temperature fields are also shown. The tracer response curve shows two distinct peaks, indicating the existence of at least two preferential paths along the fracture, which is confirmed by the corresponding flow rate field.

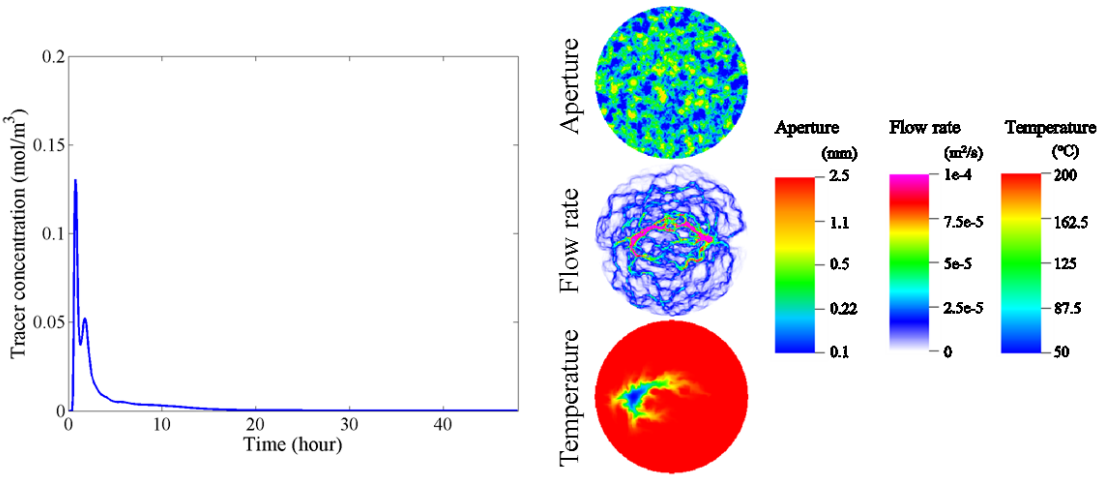


**Figure 3: Tracer response curve and the corresponding aperture, flow rate, and temperature fields from the example in Figure 2. The following figures of aperture, flow rate, and temperature fields all use the same colorbars.**

We define two metrics to quantify the tracer response curve in order to compare the tracer signatures from different realizations. One metric is the highest peak concentration. In Figure 3, the first peak has the highest tracer concentration (0.175 mol/m$^3$), and it is corresponding to the primary preferential path carrying the largest portion of flow shown in purple in the flow rate visualization in Figure 3. Unless explicitly indicated otherwise, "peak concentration" refers to the value for the highest peak concentration in this work, although multiple peaks could co-exist in the same tracer response. Greater peak concentration generally indicates more direct and shorter dominant preferential path along the fracture. The other potentially useful metric is the mean residence time $\tau$, which quantifies the average time for a tracer particle to travel from the injection well to the production well, mathematically defined as

$$\tau = \frac{\int_{t=0}^{\infty} tC\,dt}{\int_{t=0}^{\infty} C\,dt} \tag{7}$$

### 4.2 Tracer response curves and long-term performance

In this section, we investigate the relationship between features in the tracer response curves and the long-term performance for selected representative aperture fields. As the effectively production life and the amount of useable heat are closely correlated (Guo et al. 2016), we use production life as the only metric for reservoir performance. Figure 4 shows the tracer response curves and the evolutions of aperture, flow rate, and temperature fields from two representative realizations. The upper case has a relatively short production life, and the lower one has a much longer production life. Even though the two aperture fields share the same mean aperture, aperture standard deviation, and correlation length of aperture field, the production lives are very different (5 years vs. beyond 30 years). The tracer response curves also show distinct characteristics correspondingly. The curve for the upper realization has a high peak concentration and the highest peak occurs at an early time. This indicates a short and dominant preferential path along the fracture, which is confirmed by the purple region on the flow rate figure after 3 months. The short dominant preferential path leads to a relatively small heat exchange area and further flow channelization through thermo-mechanical processes. On the other hand, the tracer response curve for the lower case has a much smaller peak concentration and the multiple peaks occur at relatively late times. This indicates a more diffusive flow pattern than that in the upper realization, which can also be confirmed by comparing the flow rate fields after 3 months in both realizations. The diffusive flow pattern enables a longer production life because the heat exchange area is greater and the further flow channelization is weaker than those with a short dominant preferential path.

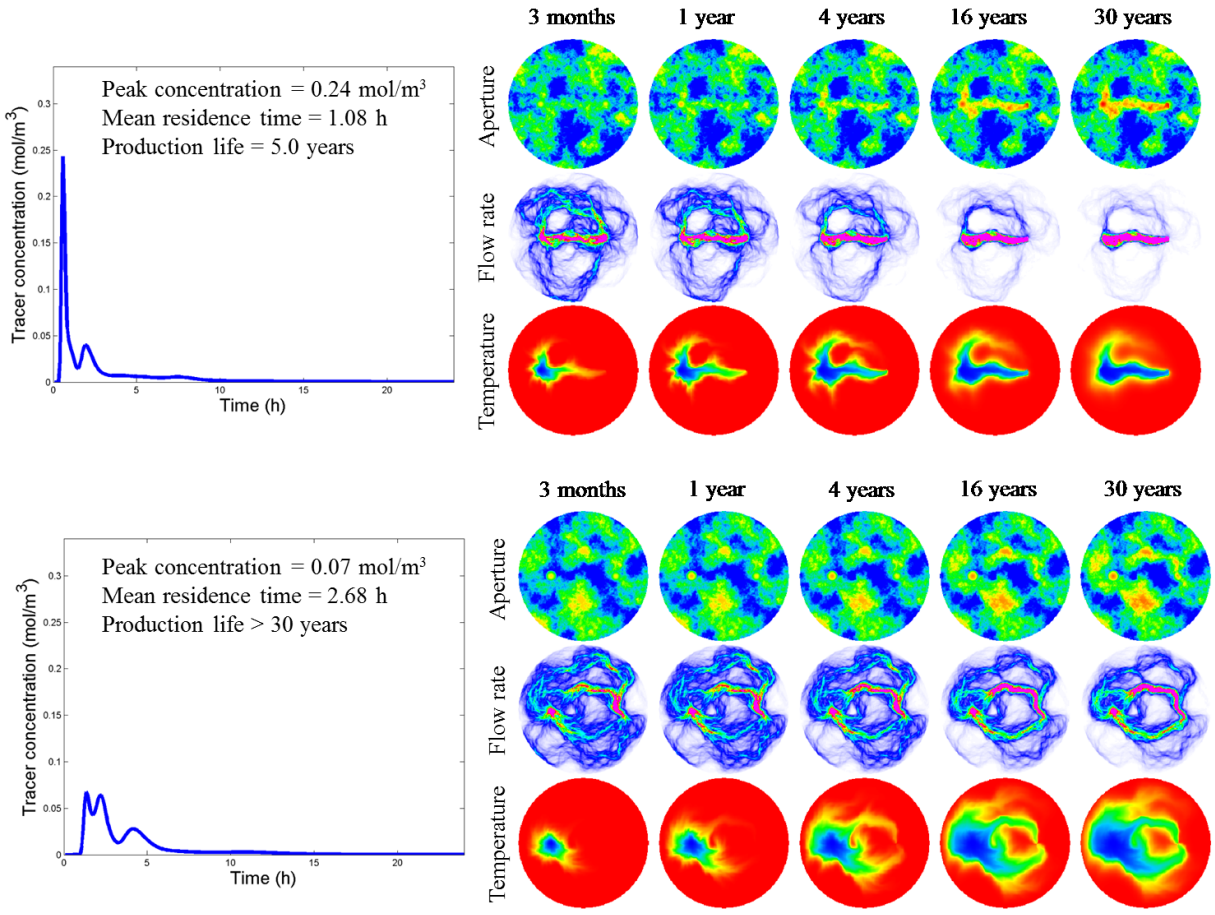


**Figure 4: Tracer response curves and the evolutions of aperture, flow rate, and temperature fields from two representative realizations with correlation length of 200 m and standard deviation of 0.17 mm.**

Figure 5 shows the tracer response curves and the evolutions of aperture, flow rate, and temperature fields from a highly idealized case with a homogeneous aperture field, and also a representative case with a correlation length of 12.5 m and a standard deviation of 0.17 mm. Similar to what we observed in the previous study, the tracer response curves from the aperture fields with a short correlation length look like the tracer response curve from a homogeneous aperture field.

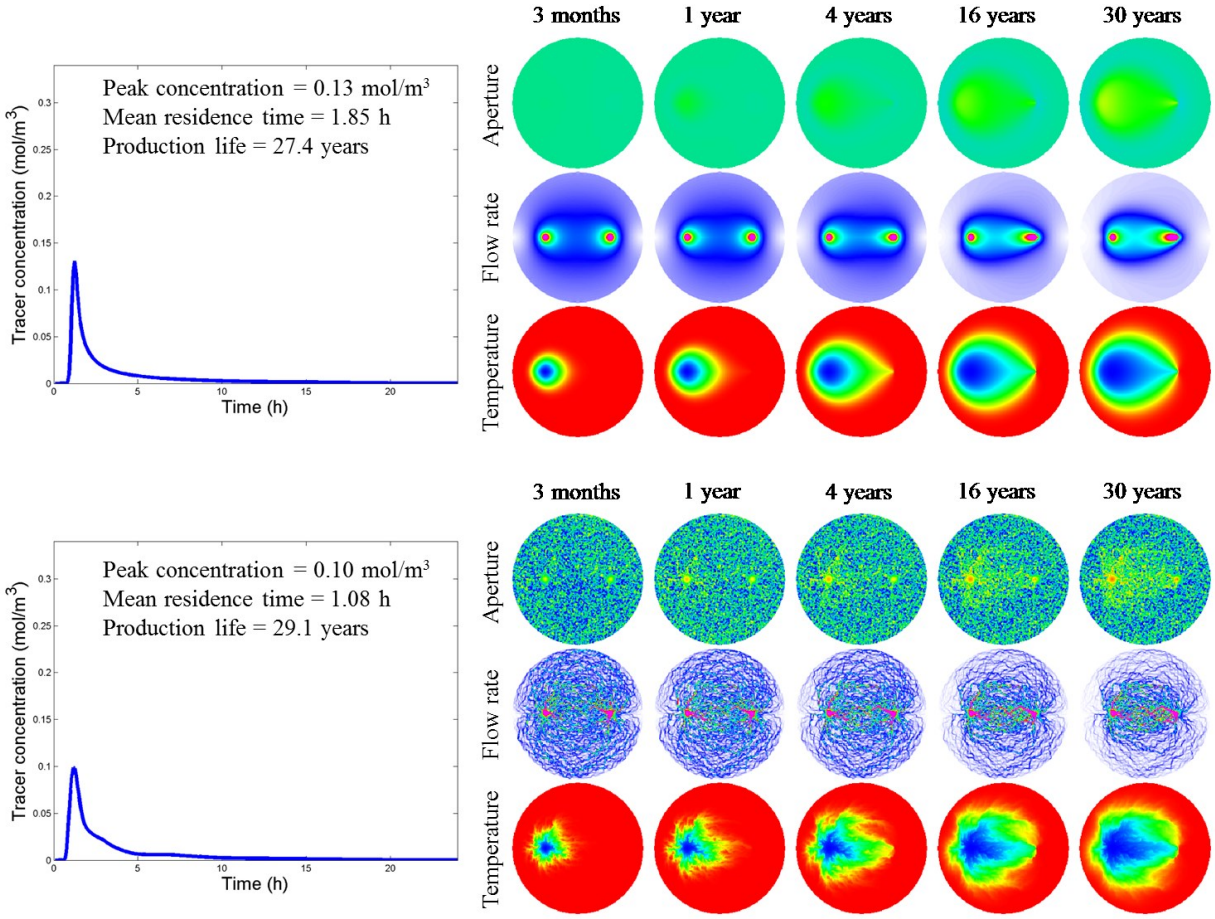


**Figure 5: Tracer response curves and the evolutions of aperture, flow rate, and temperature fields from the base case with homogeneous aperture and a representative realizations with correlation length of 12.5 m and standard deviation of 0.17 mm.**

Figure 6 shows the results from two representative realizations with correlation length of 200 m and standard deviation of 0.68 mm. Guo et al. (2016) showed that such long correlation lengths and large standard deviations of the aperture field generally lead to highly variable reservoir performances. Again, we present two random realizations with relatively poor and good performance, respectively. The comparison confirms the observation that an aperture field dominated by a short dominant preferential path is associated with tracer responses with an early and high peak concentration. The heat production performance of such a fracture is generally poor. On the other hand, a fracture enabling multiple flow paths (relatively diffusive flow field, generally better-performing) is associated with a tracer signature of low peak concentration and late peak(s).

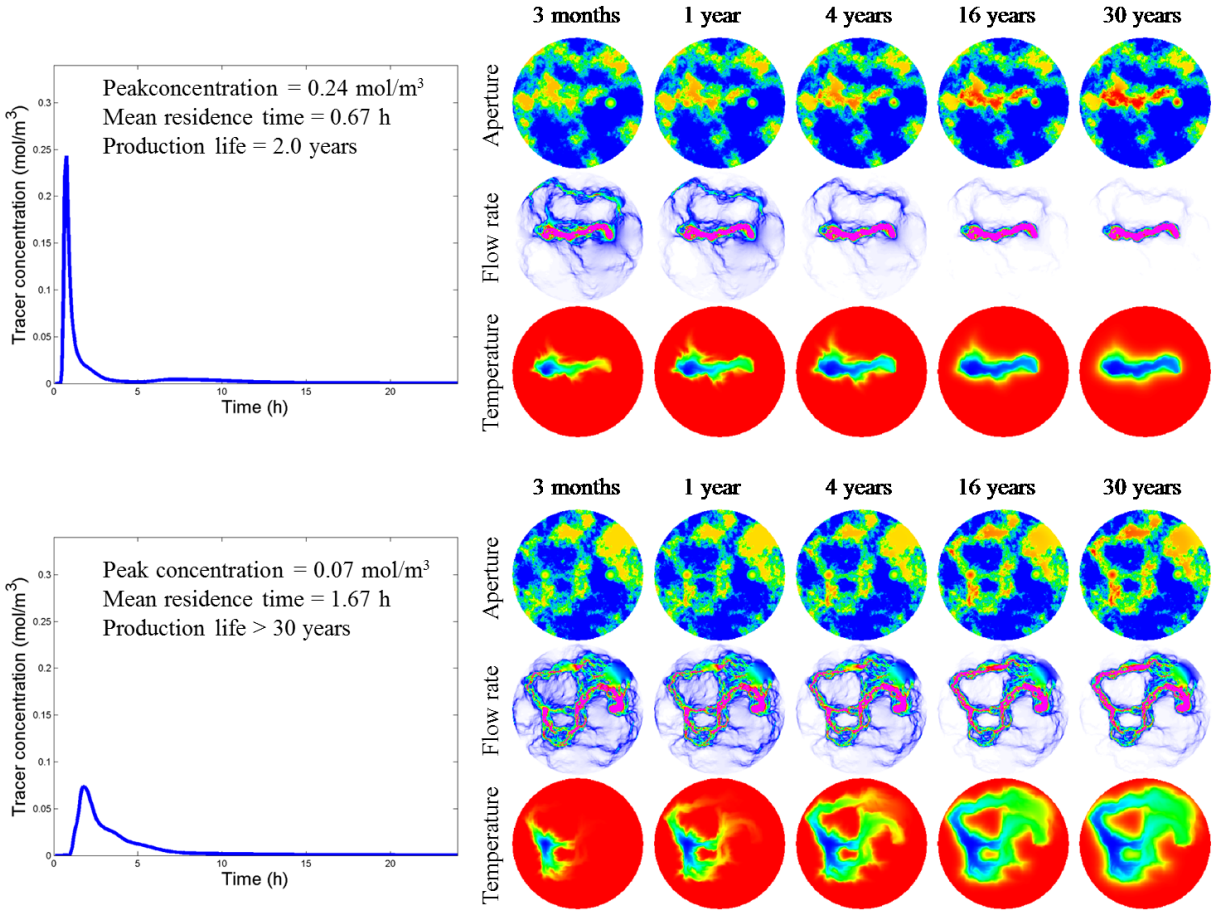


**Figure 6: Tracer response curves and the evolutions of aperture, flow rate, and temperature fields from two representative realizations with correlation length of 200 m and standard deviation of 0.68 mm.**

### 4.3 Correlation between tracer metrics and heat production life

The main purpose of the representative examples presented in the previous section was to identify the mostly salient tracer signatures of highly channelized flow fields and those of more diffusive flow fields. Therefore, we selected relative extreme cases for that purpose. In this section, we pool the tracer and heat production results for all the 200 realizations and investigate the correlation between two tracer metrics and simulated production lives. Figure 7 shows the correlation between the peak tracer concentrations and the heat production lives. The results of varying correlation length (Set 1 in section 3.2) are summarized in the left figure, and the results of varying standard deviation (Set 2 in section 3.2) are shown in the right figure. Each circle represents the results from one random realization, and we use different colors to group the circles with the same correlation length or standard deviation on the two sub-figures. An overall negative correlation between the production life and the peak concentration is observed, and the correlation is stronger for high peak concentration cases (poor heat production performance) and weaker for cases with better heat production performance. The observation shows that high peak tracer concentration values are generally indicative of poor heat production performance, but the metric does not have much predictive power for cases with better performance. Figure 8 shows the correlation between the mean residence times and production lives from realizations with varying correlation length (left figure) and varying standard deviation (right figure). Again, the production life is likely to be short when the mean residence time is short, and the production life is not strongly correlated with the mean residence time for long mean residence times. This observation is similar to that from Figure 7. Using the mean tracer residence time, we can identify reservoirs with poor performance but cannot distinguish the good-performance reservoirs from the intermediate-performance reservoirs.

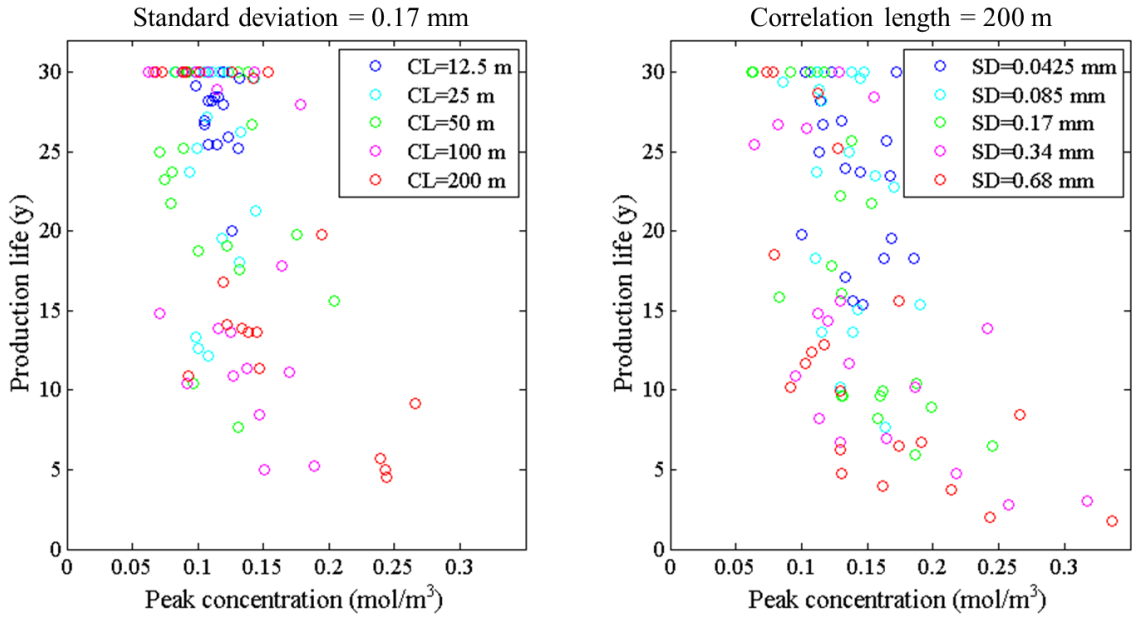


**Figure 7: Correlation between the peak concentrations of tracer tests and the production lives of all the realizations.**

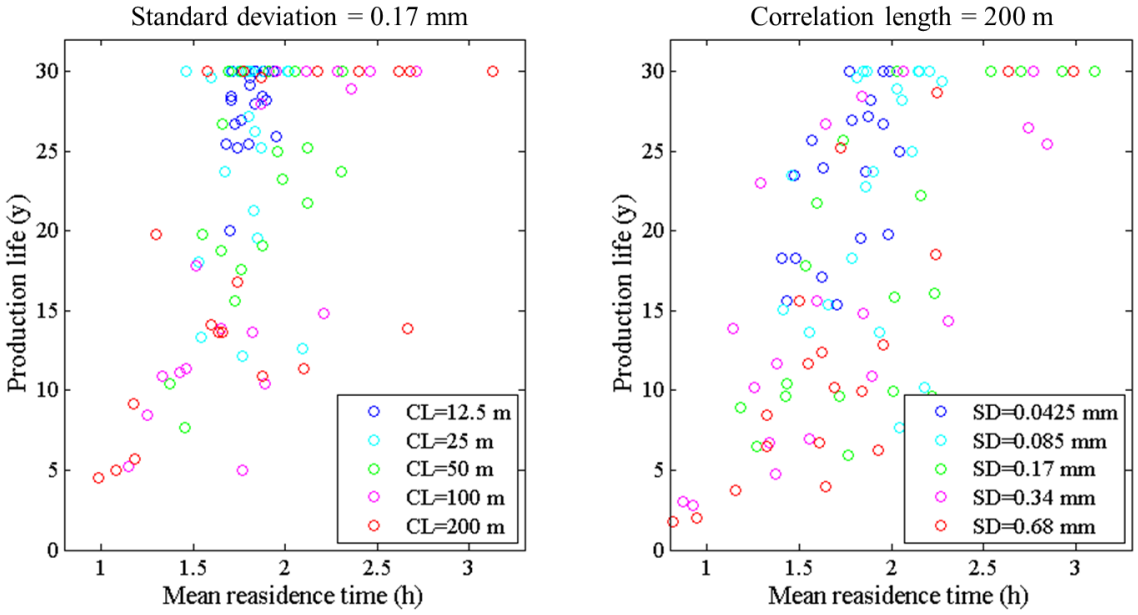


**Figure 8: Correlation between the mean residence times and the production lives of all the realizations. CL is short for correlation length and SD is short for standard deviation.**

## 5. CONCLUDING REMARKS

Based on our previously developed THM model for the study of flow channeling in fracture-dominated EGS reservoirs, a conservative tracer transport model was developed to simulate tracer tests. We investigated the possibility of using early-stage tracer tests to predict long-term reservoir performance. We found that the tracer response curve could be a useful indicator for flow field characteristics along the fracture: A fracture dominated by a single major preferential flow path tends to result in an early and great peak tracer concentration, whereas a fracture that features a more diffusive flow field tends to have later and lower peak concentration. However, although both the peak tracer concentration and the mean residence time can identify flow fields that lead to very poor heat production performance, they cannot adequately differentiate between good-performance and intermediate-performance systems. This is mainly due to an intrinsic limitation of using early-stage flow field signatures to predict long-term performance. If a fracture enables a short and direct major flow path in the beginning of the heat production, there is hardly any mechanism that can naturally alter the flow field into a more diffusive one, so poor performance is inevitable and relatively easily predictable for this scenario. As shown in Guo et al. (2016), the diffusivity of the flow field along a fracture can change significantly during the course of the heat production, primarily due to thermo-mechanical coupling. Typically, diffusivity of the flow field decreases as flow channeling becomes exacerbated. Many fractures with

initially diffusive flow fields can eventually deliver poor performance due to the development of short flow channels. Whether such secondary flow channeling would occur to a fracture is dependent on many factors other than the original diffusivity itself. The diffusivity of the initial flow field is therefore inadequate for predicting long-term heat production performance. Further study is needed to investigate the opportunity to use reactive tracers, such as matrix sorptive tracers, to get more information about flow channeling and infer reservoir performance. Also note that all the virtual reservoirs/fractures included in the current study have the same mean aperture. Although a change in the mean aperture alone does not change the heat exchange surface area available to the EGS, it can have direct and significant influences on the tracer metrics investigated in this work. Therefore, some kind of normalization schemes will be necessary in order to generalize the criteria for evaluating tracer metrics in subsequent, more comprehensive studies.

**Acknowledgement**

The authors gratefully acknowledge the Geothermal Technologies Program of the US Department of Energy for support of this work under the Enhanced Geothermal Systems Program. The authors also would like to acknowledge their collaborators at the Lawrence Livermore National Laboratory. This work was performed under the auspices of the U.S. Department of Energy by Lawrence Livermore National Laboratory under Contract DE-AC52-07NA27344 (LLNL-CONF-682357).

**References**

Axelsson, G., Flovenz, O. G., Hauksdottir, S., Hjartarson, A., Liu, J. (2001). "Analysis of Tracer Test Data, and Injection-Induced Cooling, in the Laugaland Geothermal Field, N-Iceland." Geothermics, 30(6), 697-725.

Ayling, B. F., Hogarth, R. A., Rose, P. E. (2015). "Tracer Testing at the Habanero EGS Site, Central Australia." Geothermics.

Bloomfield, K. K., and Moore, J. N. (2003). "Modeling Hydrofluorocarbon Compounds as Geothermal Tracers." Geothermics, 32(3), 203-218.

Fu, P., Hao, Y., Walsh, S. D. C., Carrigan, C. R. (2015). "Thermal Drawdown-Induced Flow Channeling in Fractured Geothermal Reservoirs." Rock Mech Rock Eng. 1-25.

Gale, J., Macleod, R., Welham, J., Cole, C., Vail, L. (1987). "Hydrogeological Characterization of the Stripa Site." Nationale Genossenschaft fuer die Lagerung Radioaktiver Abfaelle (NAGRA)

Guo, B., Fu, P., Hao, Y., Peters, C. A., Carrigan, C. R. (2016). "Thermal Drawdown-Induced Flow Channeling in a Single Fracture in EGS." Geothermics, 61, 46-62.

Hadermann, J., and Heer, W. (1996). "The Grimsel (Switzerland) Migration Experiment: Integrating Field Experiments, Laboratory Investigations and Modelling." J. Contam. Hydrol., 21(1), 87-100.

Hogarth, R. A., and Bour, D. (2015). "Flow Performance of the Habanero EGS Closed Loop." Proc., World Geothermal Congress, Melbourne, Australia

Horne, R. (1985). "Reservoir Engineering Aspects of Reinjection." Geothermics, 14(2), 449-457.

Kumagai, N., Tanaka, T., Kitao, K. (2004). "Characterization of Geothermal Fluid Flows at Sumikawa Geothermal Area, Japan, using Two Types of Tracers and an Improved Multi-Path Model." Geothermics, 33(3), 257-275.

Llanos, E. M., Zarrouk, S. J., Hogarth, R. A. (2015). "Numerical Model of the Habanero Geothermal Reservoir, Australia." Geothermics, 53, 308-319.

Maier, F., Schaffer, M., Licha, T. (2015). "Determination of Temperatures and Cooled Fractions by Means of Hydrolyzable Thermo-Sensitive Tracers." Geothermics, 58, 87-93.

McGuire, P., Chatham, J., Paskvan, F., Sommer, D., Carini, F. (2005). "Low salinity oil recovery: An exciting new EOR opportunity for alaska's north slope." Proc., SPE Western Regional Meeting, Society of Petroleum Engineers.

Nottebohm, M., Licha, T., Sauter, M. (2012). "Tracer Design for Tracking Thermal Fronts in Geothermal Reservoirs." Geothermics, 43, 37-44.

Radilla, G., Sausse, J., Sanjuan, B., Fourar, M. (2012). "Interpreting Tracer Tests in the Enhanced Geothermal System (EGS) of Soultz-Sous-Forêts using the Equivalent Stratified Medium Approach." Geothermics, 44, 43-51.

Rose, P. E., Benoit, W. R., Kilbourn, P. M. (2001). "The Application of the Polyaromatic Sulfonates as Tracers in Geothermal Reservoirs." Geothermics, 30(6), 617-640.

Sanjuan, B., Pinault, J., Rose, P., Gérard, A., Brach, M., Braibant, G., Crouzet, C., Foucher, J., Gautier, A., Touzelet, S. (2006). "Tracer Testing of the Geothermal Heat Exchanger at Soultz-Sous-Forêts (France) between 2000 and 2005." Geothermics, 35(5), 622-653.

Tsang, C., and Neretnieks, I. (1998). "Flow Channeling in Heterogeneous Fractured Rocks." Rev. Geophys., 36(2), 275-298.

Tsang, Y., and Tsang, C. (1989). "Flow Channeling in a Single Fracture as a two-dimensional Strongly Heterogeneous Permeable Medium." Water Resour. Res., 25(9), 2076-2080.

Wu, X., Pope, G. A., Shook, G. M., Srinivasan, S. (2008). "Prediction of Enthalpy Production from Fractured Geothermal Reservoirs using Partitioning Tracers." Int. J. Heat Mass Transfer, 51(5), 1453-1466.